

Table of Contents

NMR SPECTRA	2
S1	2
S2	3
S3	4
IR SPECTRA	5
S4	5
S5	5
S6	6
MASS SPECTRA	6
S7	6
S8	7
S9	8
S10	9
COMPUTATIONAL	10
S11	10
S12	11
S13	12
CRYSTAL STRUCTURE	13
Table S1	13
S14	14
PXRD	14
S15	14

NMR SPECTRA

S1

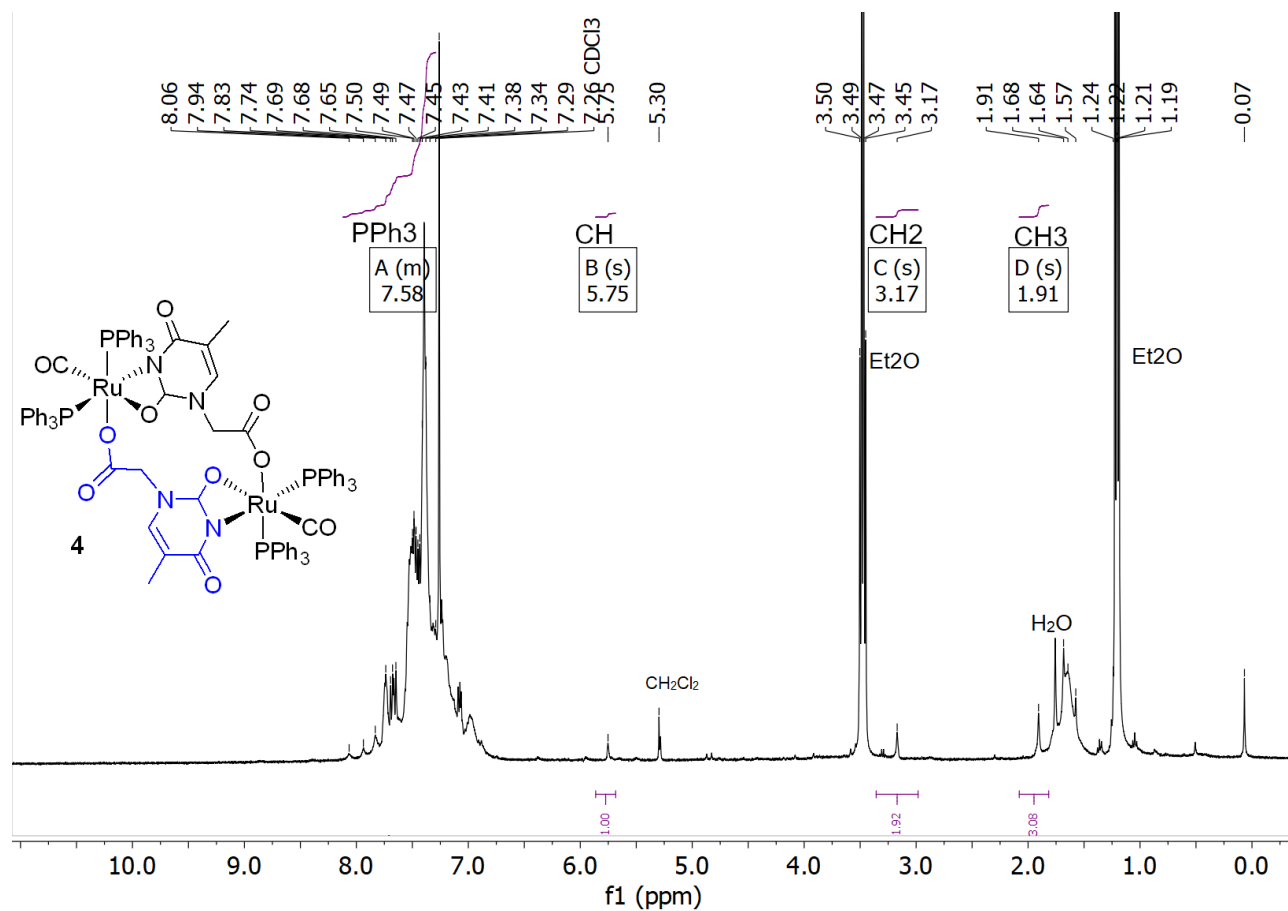
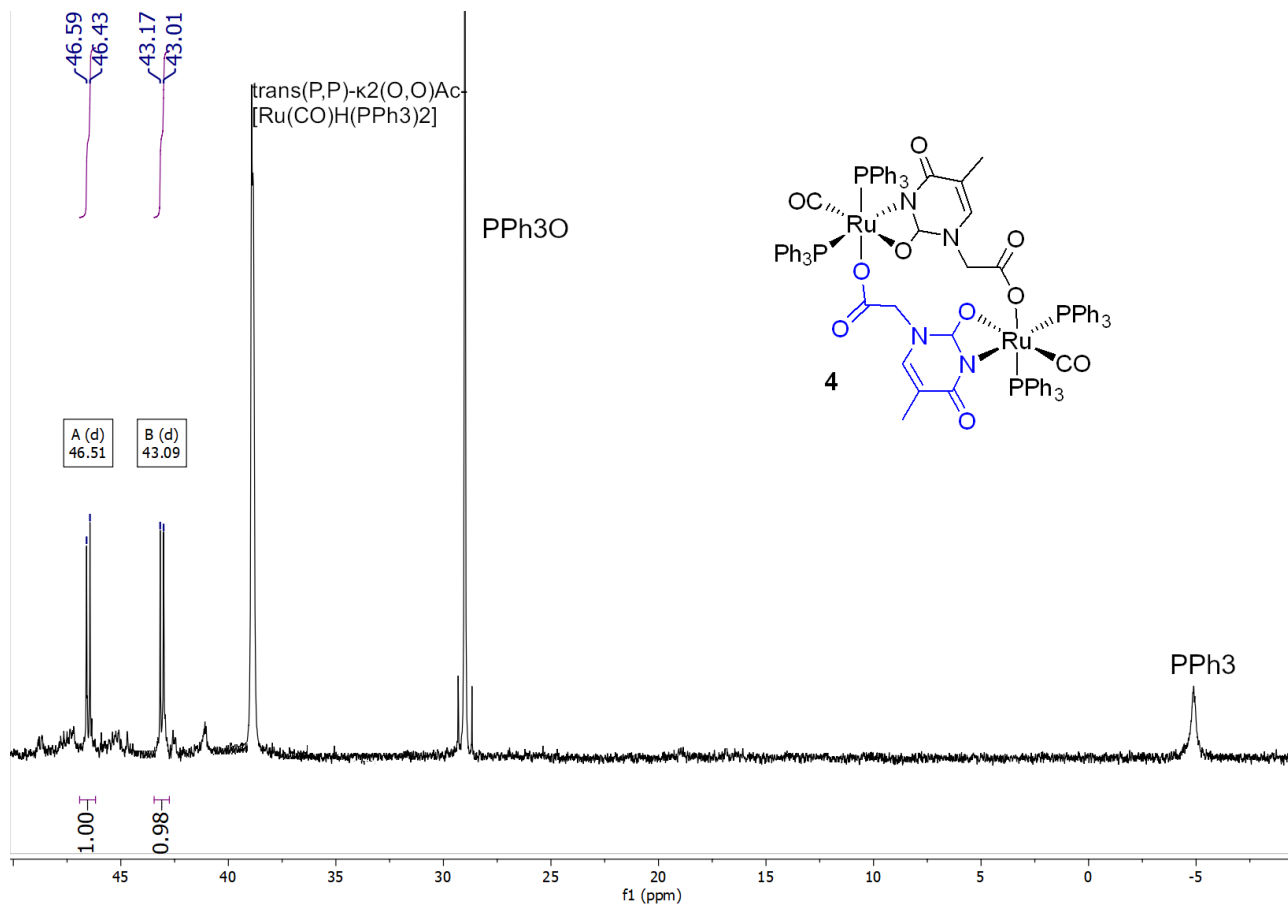


Figure S1: ¹H NMR spectrum of 4 in CDCl₃ (300 Mhz)

S2

Figure S2: ³¹P NMR spectrum of **4** in CDCl₃ (162 Mhz)

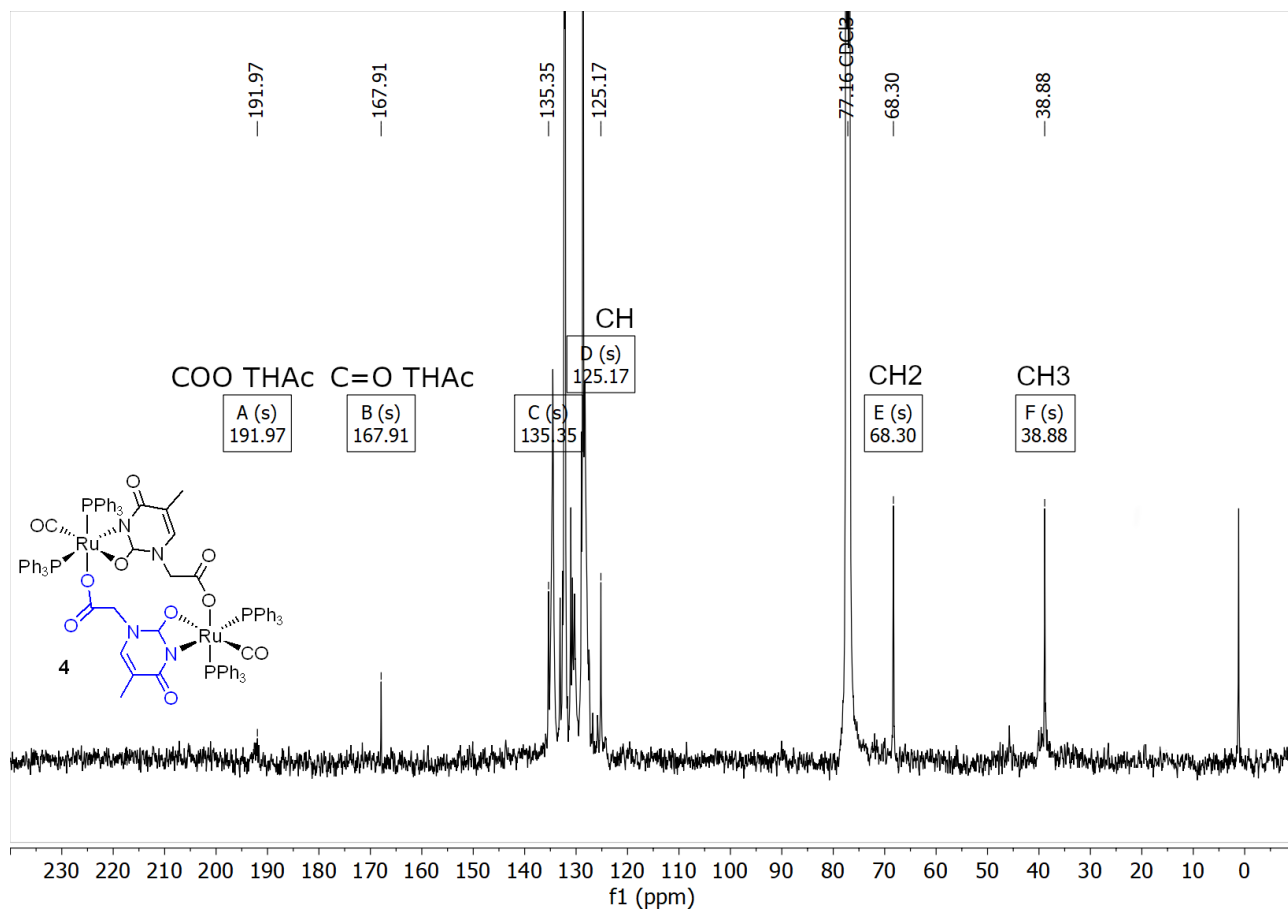


Figure S3: ¹³C NMR spectrum of 4 in CDCl₃ (101 Mhz)

IR SPECTRA

S4

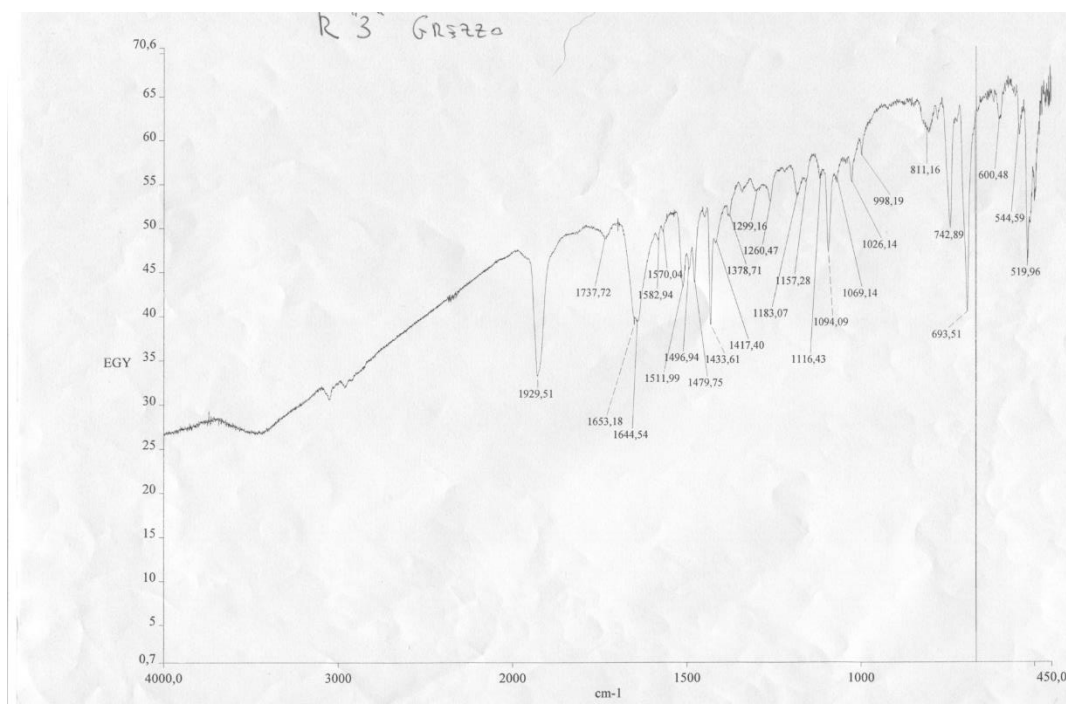


Figure S4: IR spectrum of k 1 (O)-2a enolic form. The band at 1511 cm-1 is attributable to the incipient transformation to the enol moiety of the precursor of 4.

S5

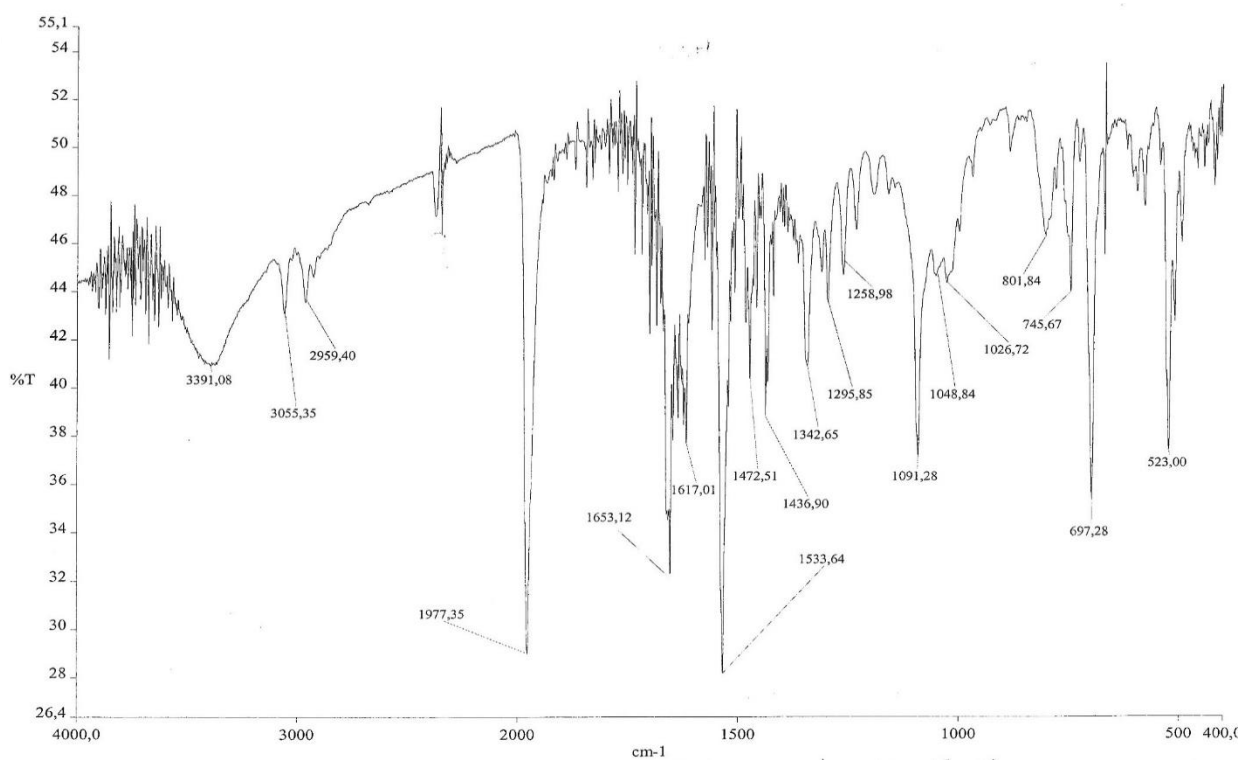
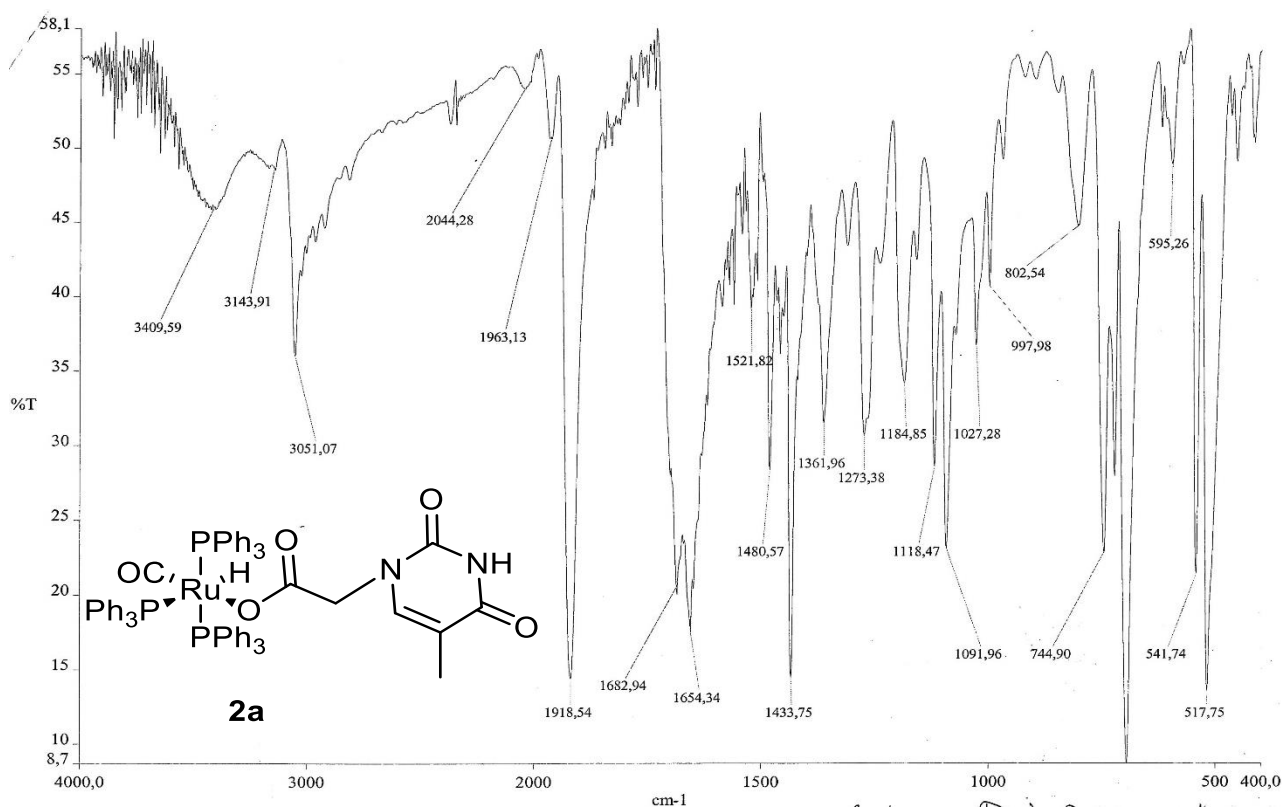


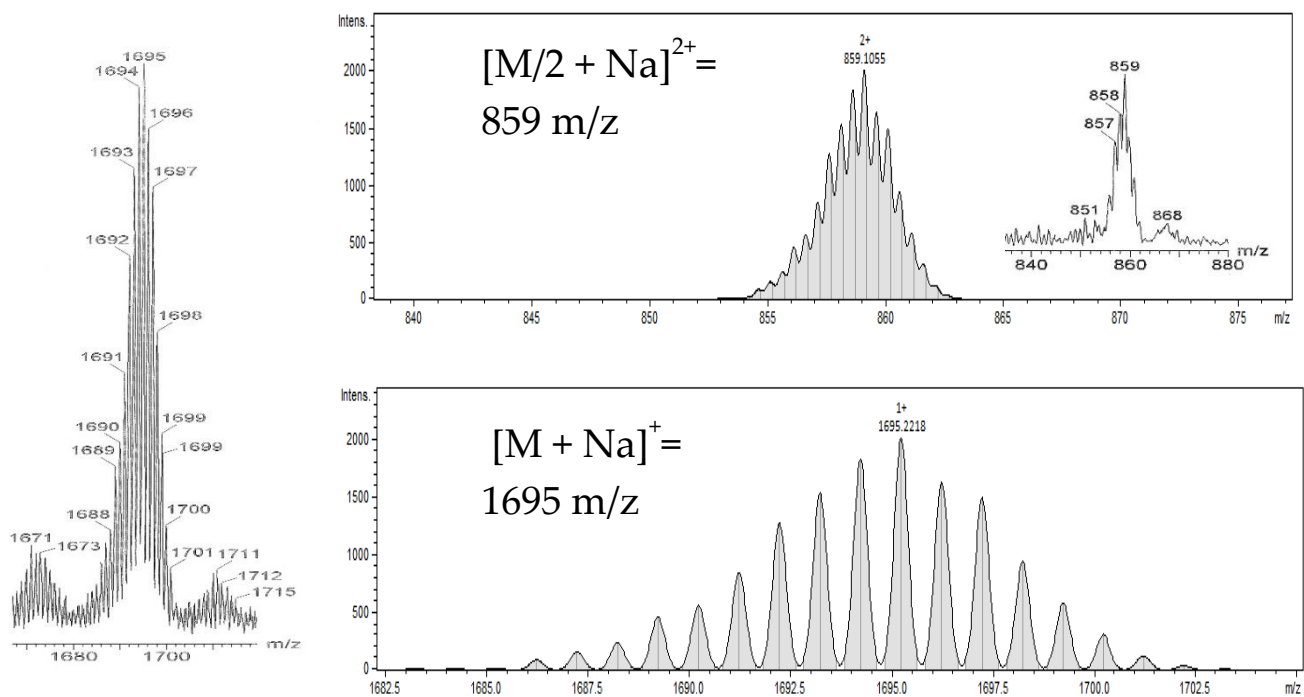
Figure S5: IR spectrum of microcrystalline powder 4 of a different preparation: the band at $\nu = 1533.64$ is characteristic for the lactim tautomeric form.

S6

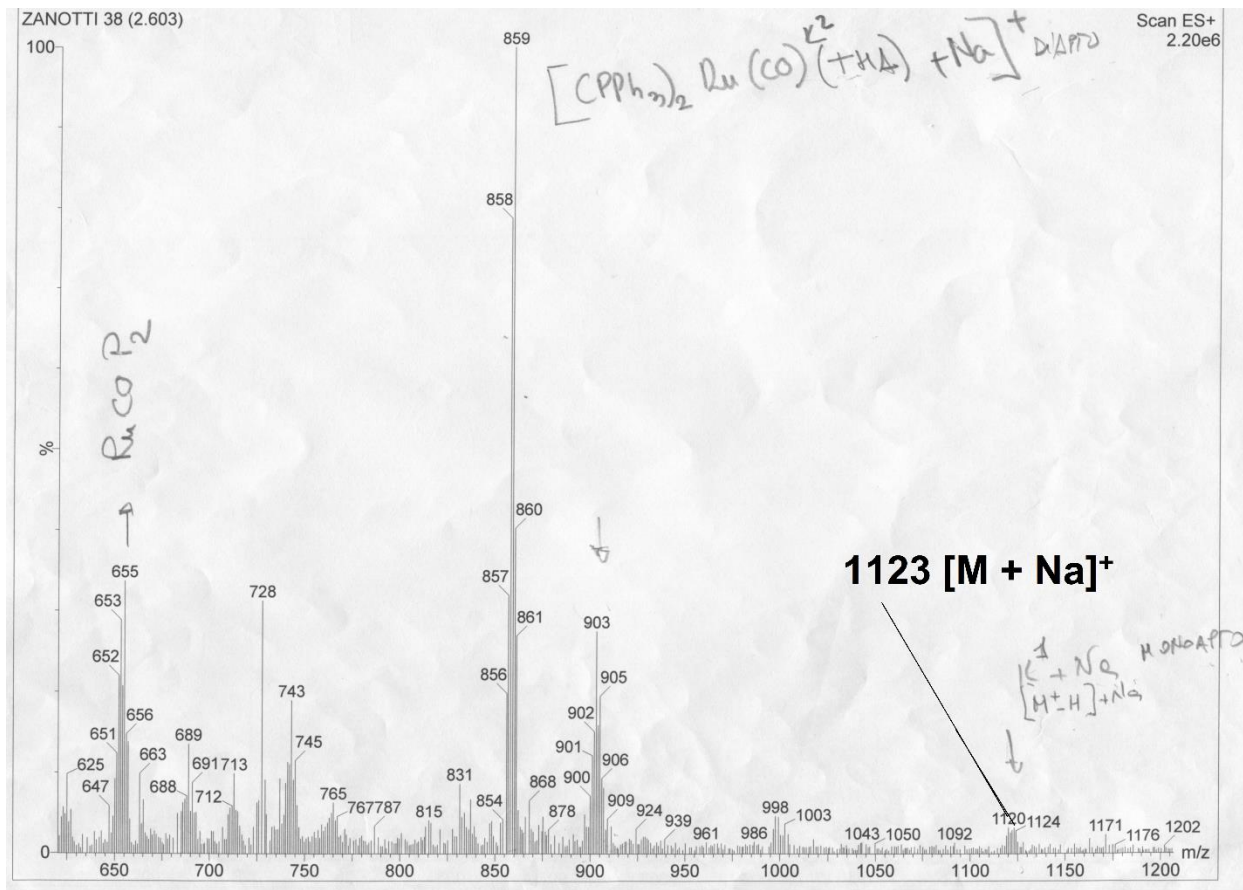
Figure S6: IR spectrum of KETO **2a**, after extraction in DCM/Et₂ 1:1

MASS SPECTRA

S7

Figure S7: Mass spectrum of **4** compared to simulations.

A



B

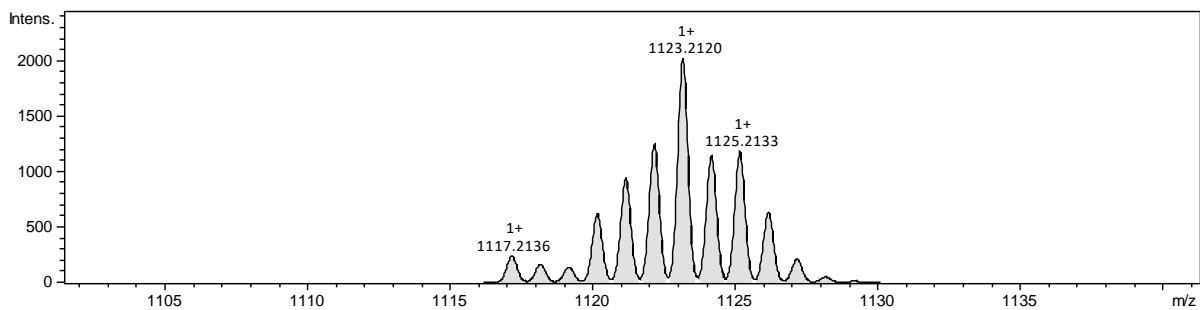


Figure S8: (A) Mass spectrum of $k^1(O)$ -2a. (B) simulation of $[M + Na]^+$

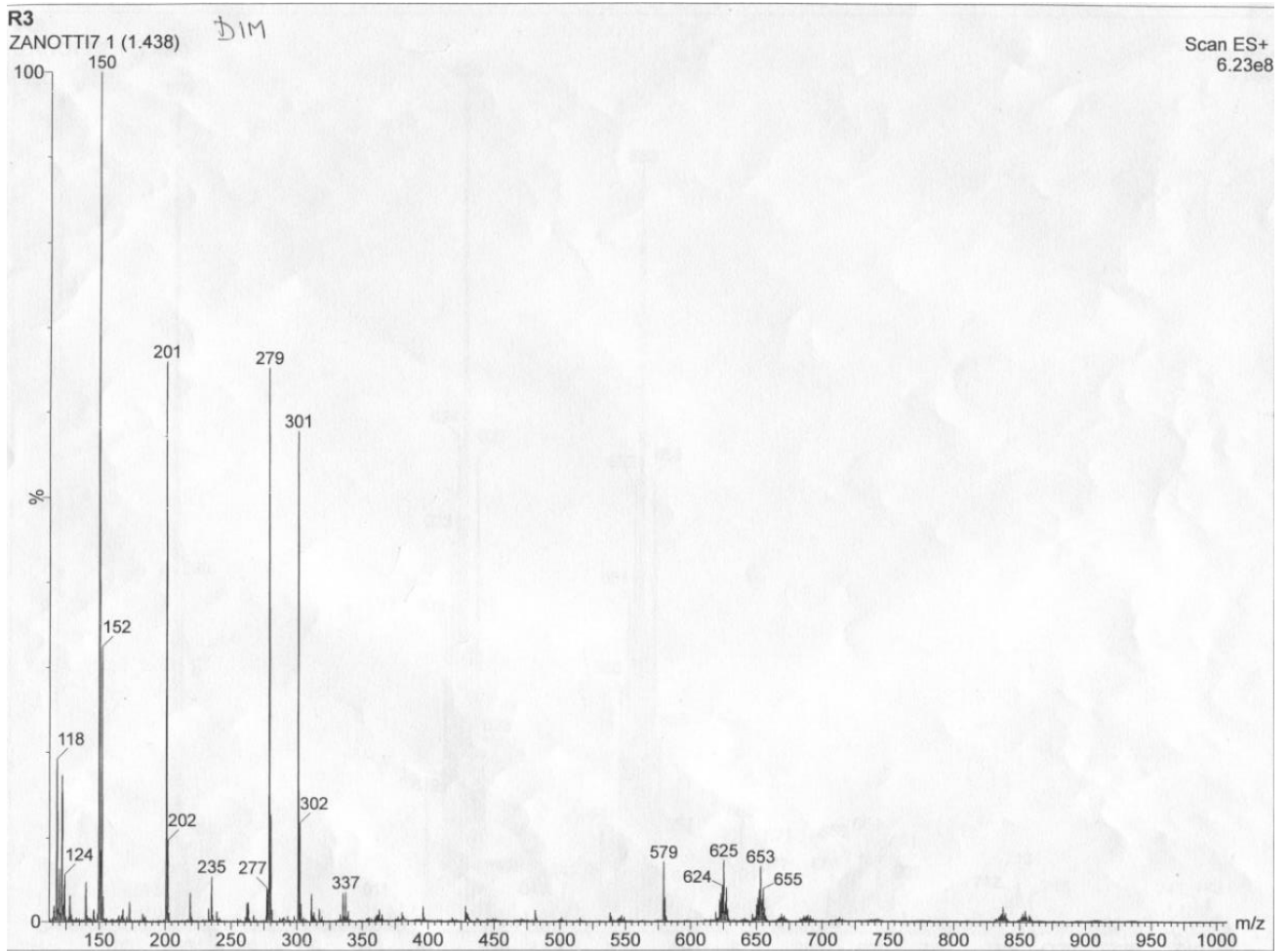
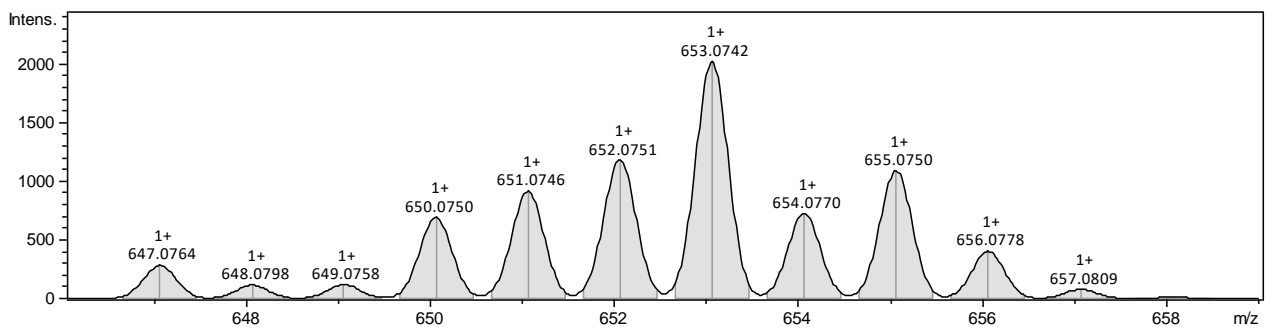
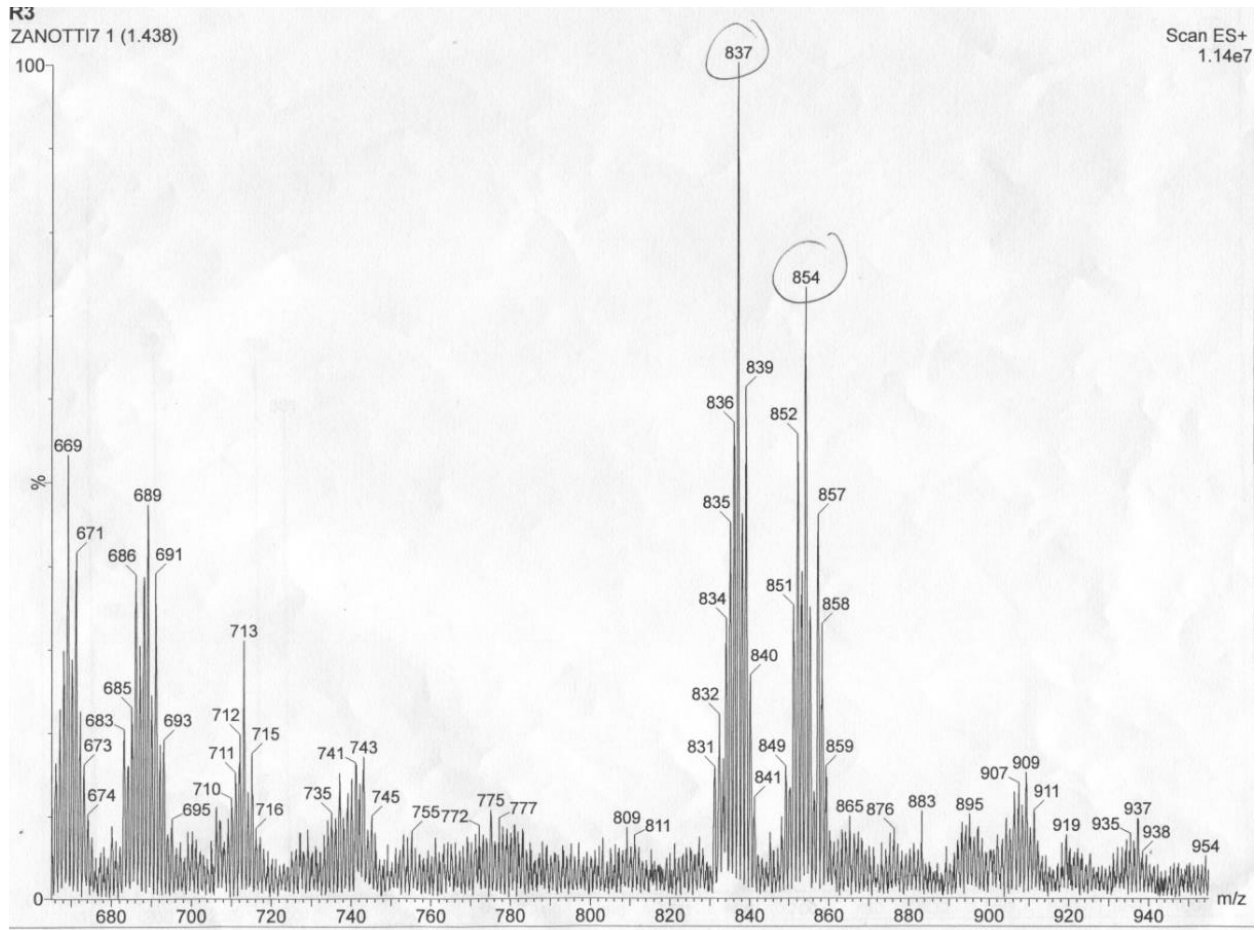
A**B**

Figure S9: (A) Mass spectrum of $k^2(O,O)$ -3 (positive mode). (B) simulation of $[M - THAc]^+$

S10

A



B

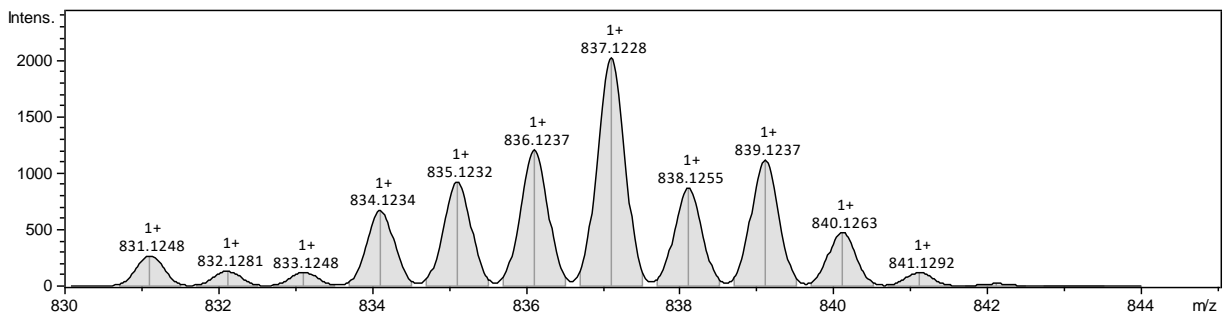


Figure S10: (A) Mass spectrum of $k^2(O,O)$ -3 (positive mode, m/z : 680 – 940). (B) Simulation of $[M - H]^+$

COMPUTATIONAL

S11

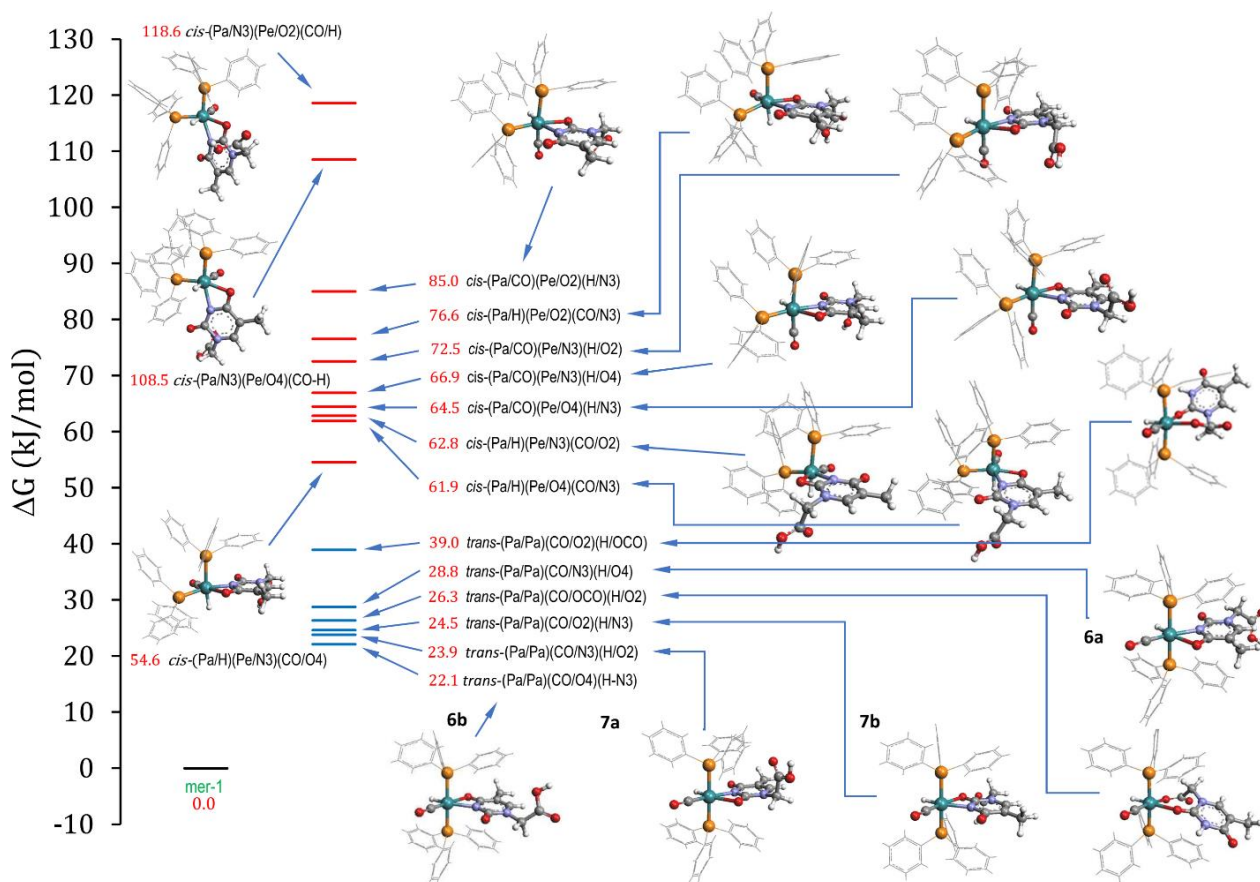


Figure S11: DFT calculations of all four membered- $k_2(N,O)$ - heteroleptic and $k_2(O,O)$ - heptacycles. All energies are calculated relative to the energy of mer-1 + thymine-acetic acid reactants. All species are named using the following scheme: the three couples of ligands at opposite vertex of the octahedron are enclosed in parentheses, with the additional specification of relative phosphine position. Legend: Pa=axial phosphine, Pe=equatorial phosphine, CO=carbonyl, H=hydride, OCO=thymine carboxylate, O2=thymine oxygen in 2 position, N3=thymine nitrogen in 3 position, O4=thymine oxygen in 4 position

S12

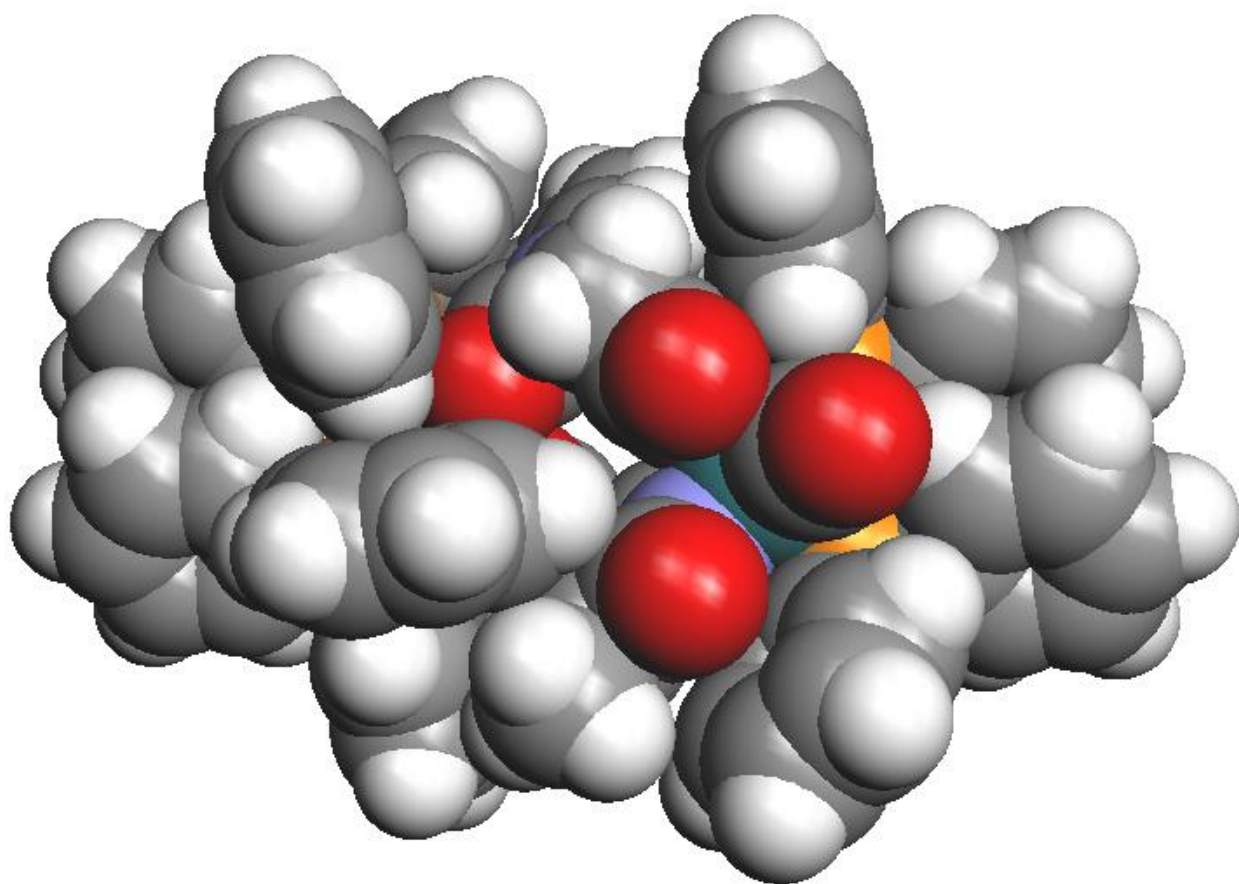


Figure S12: Space filling of 4

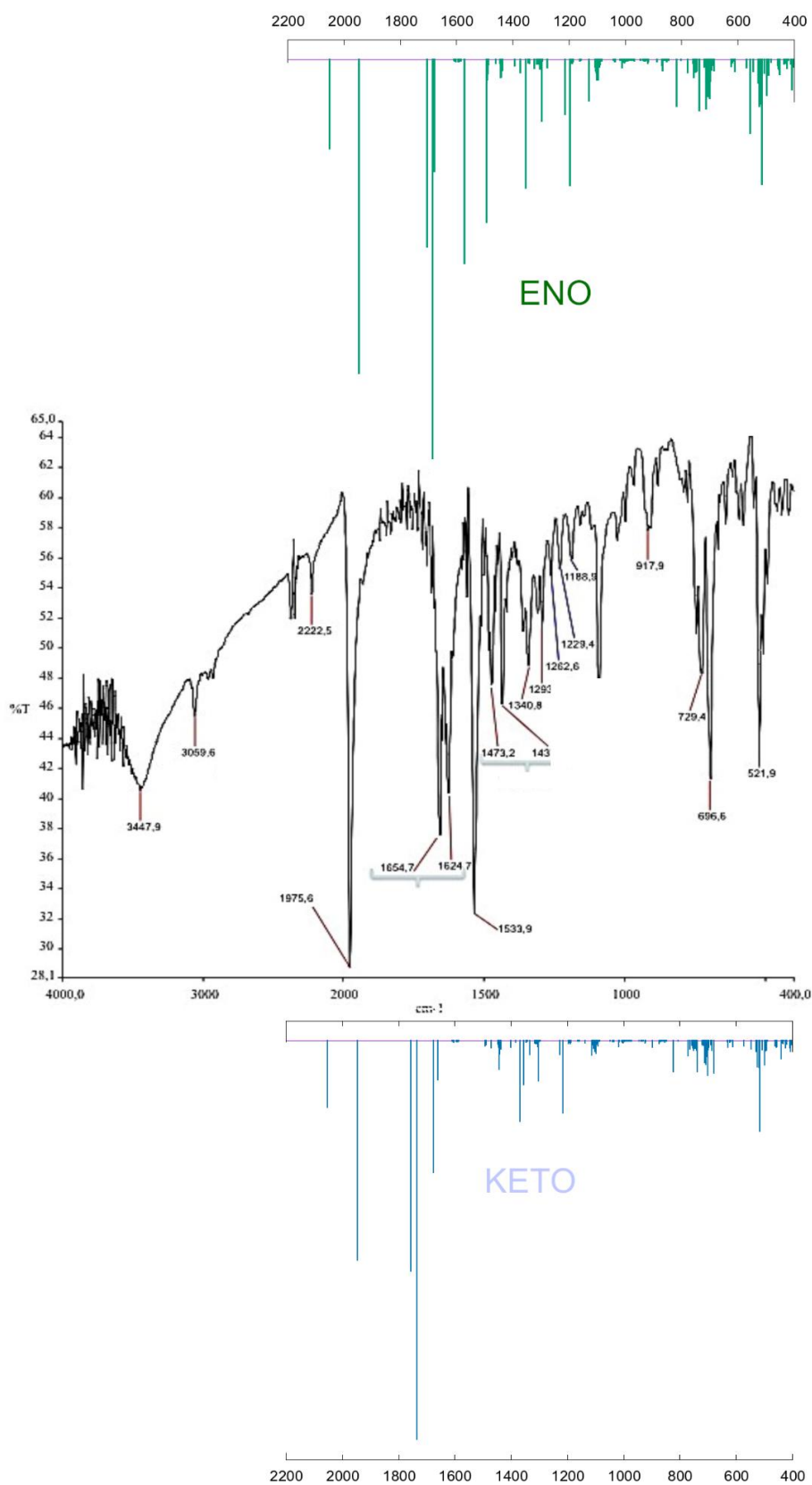


Figure S13: Comparison between the experimental IR spectrum of DFT-simulated IR spectra of keto and Enol form relative to the dimer 4.

CRYSTAL STRUCTURE

Table S1

Table S1. Crystal data and experimental details for **4**

Compound	4
Formula	C ₈₈ H ₇₂ N ₄ O ₁₀ P ₄ Ru ₂ .2CHCl ₃ .2H ₂ O
Fw	1942.25
T, K	296(2)
λ , Å	0.71073
Crystal symmetry	Monoclinic
Space group	P2 ₁ /c
<i>a</i> , Å	10.220(2)
<i>b</i> , Å	29.771(7)
<i>c</i> , Å	14.713(3)
α	90
β	90.005(2)
γ	90
Cell volume, Å ³	4476.7(17)
Z	2
D _c , Mg m ⁻³	1.441
μ (Mo-K α), mm ⁻¹	0.649
F(000)	1976
Crystal size/ mm	0.15 x 0.05 x 0.05
θ limits, °	1.368 to 25.000
Reflections collected	36382
Unique obs. Reflections [F _o > 4 σ (F _o)]	7816 [R(int) = 0.1264]
Goodness-of-fit-on F ²	0.983
R ₁ (F) ^a , wR ₂ (F ²) [I > 2 σ (I)] ^b	0.0738, 0.1418
Largest diff. peak and hole, e. Å ⁻³	0.773 and -0.616

^aR₁ = $\sum ||F_o| - |F_c|| / \sum |F_o|$. ^bwR₂ = $[\sum w(F_o^2 - F_c^2)^2 / \sum w(F_o^2)^2]^{1/2}$ where $w = 1 / [\sigma^2(F_o^2) + (aP)^2 + bP]$ where $P = (F_o^2 + F_c^2) / 3$.

S14

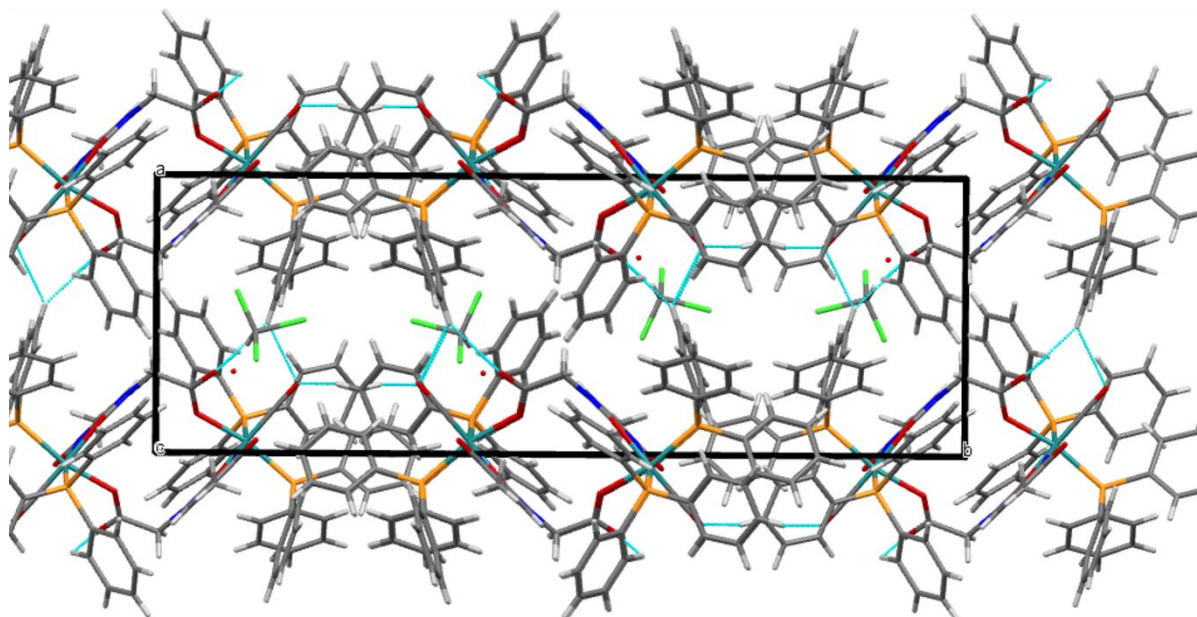


Figure S14: View down the c axis of the crystal packing of 4. Light blue dotted lines represent H bonding interactions.

PXRD

S15

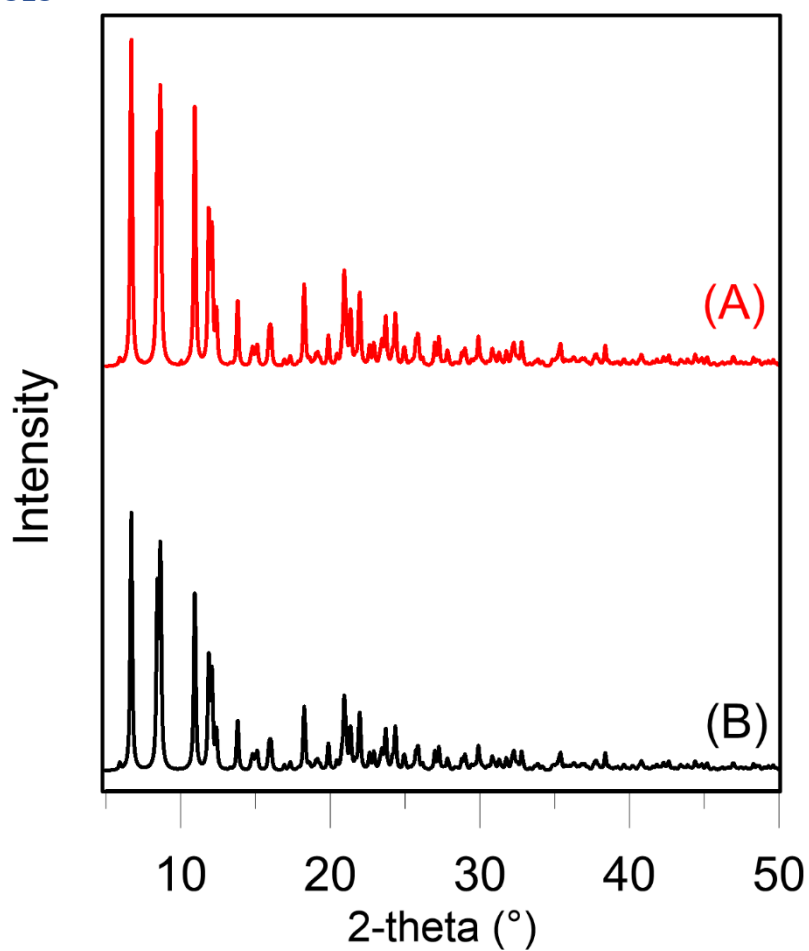


Figure S15: Comparison between the experimental (A) and simulated (B) PXRD spectra of 4, which supports the phase purity of compound 4.